THE JOURNAL OF BIOLOGICAL CHEMISTRY VOL. 284, NO. 25, pp. 16860–16871, June 19, 2009

Decreased Expression of Cholesterol 7α-Hydroxylase and Altered Bile Acid Metabolism in *Apobec-1*$^{-/-}$ Mice Lead to Increased Gallstone Susceptibility*[S]

Received for publication, February 12, 2009, and in revised form, April 17, 2009 Published, JBC Papers in Press, April 22, 2009, DOI 10.1074/jbc.M109.010173

Yan Xie[‡], Valerie Blanc[‡], Thomas A. Kerr[‡], Susan Kennedy[‡], Jianyang Luo[‡], Elizabeth P. Newberry[‡], and Nicholas O. Davidson[‡§1]

From the Departments of [‡]Medicine and [§]Pharmacology and Developmental Biology, Washington University School of Medicine, St. Louis, Missouri 63110

Quantitative trait mapping in mice identified a susceptibility locus for gallstones (*Lith6*) spanning the *Apobec-1* locus, the structural gene encoding the RNA-specific cytidine deaminase responsible for production of apolipoprotein B48 in mammalian small intestine and rodent liver. This observation prompted us to compare dietary gallstone susceptibility in *Apobec-1*$^{-/-}$ mice and congenic C57BL/6 wild type controls. When fed a lithogenic diet (LD) for 2 weeks, 90% *Apobec-1*$^{-/-}$ mice developed solid gallstones in comparison with 16% wild type controls. LD-fed *Apobec-1*$^{-/-}$ mice demonstrated increased biliary cholesterol secretion as well as increased cholesterol saturation and bile acid hydrophobicity indices. These changes occurred despite a relative decrease in cholesterol absorption in LD-fed *Apobec-1*$^{-/-}$ mice. Among the possible mechanisms to account for this phenotype, expression of *Cyp7a1* mRNA and protein were significantly decreased in chow-fed *Apobec-1*$^{-/-}$ mice, decreasing further in LD-fed animals. *Cyp7a1* transcription in hepatocyte nuclei, however, was unchanged in *Apobec-1*$^{-/-}$ mice, excluding transcriptional repression as a potential mechanism for decreased *Cyp7a1* expression. We demonstrated that APOBEC-1 binds to AU-rich regions of the 3′-untranslated region of the *Cyp7a1* transcript, containing the UUUN(A/U)U consensus motif, using both UV cross-linking to recombinant APOBEC-1 and *in vivo* RNA co-immunoprecipitation. *In vivo* *Apobec-1*-dependent modulation of *Cyp7a1* expression was further confirmed following adenovirus-Apobec-1 administration to chow-fed *Apobec-1*$^{-/-}$ mice, which rescued *Cyp7a1* gene expression. Taken together, the findings suggest that the AU-rich RNA binding-protein *Apobec-1* mediates post-transcriptional regulation of murine *Cyp7a1* expression and influences susceptibility to diet-induced gallstone formation.

Cholesterol gallstone disease is highly prevalent among western societies and represents a substantial and recurrent financial burden to the health care economy (1). Considerable attention has focused on the observations that gallbladder disease and cholelithiasis demonstrate familial clustering and that shared genetic factors account for a significant portion of the risk, although environmental modifiers as well as age, gender, body habitus, and ethnicity are also of major importance (reviewed in Ref. 2). However, despite intensive study over many decades, questions remain regarding the mechanisms by which biliary cholesterol becomes supersaturated, leading to the formation of cholesterol monohydrate crystals that eventually nucleate and result in gallstone formation (reviewed in Ref. 3).

Insight into the genetic factors that underlie cholesterol gallstone disease has emerged from the study of inbred mouse strains where intercrosses between gallstone-susceptible and -resistant strains have generated a comprehensive array of candidate loci through quantitative trait locus mapping, an approach that has yielded at least 23 *LITH* loci (2, 4). Among the quantitative trait loci identified through this approach is *Lith6*, a locus on mouse chromosome 6 that mapped to a region that includes *Apobec-1* as well as other genes (*Pparg* and *Slco1a1*) involved in lipid metabolism (5). *Apobec-1*, the RNA-specific catalytic deaminase of the mammalian *ApoB* (apolipoprotein B) mRNA-editing enzyme (6), mediates C to U RNA editing of intestinal *ApoB* RNA, leading to production of APOB48, the major structural protein on chylomicrons (7). In addition, mouse and rat (but not human) liver exhibit physiologically regulated *Apobec-1*-dependent *ApoB* mRNA editing accompanying a range of developmental, nutritional, and hormonal cues, resulting in the ability of murine hepatocytes to synthesize APOB100 and APOB48 in varying proportions with accompanying changes in hepatic VLDL assembly and secretion (reviewed in Ref. 7).

Several lines of evidence suggest a plausible link between the pathways that regulate hepatic VLDL assembly and secretion and those that regulate enterohepatic bile acid metabolism. These include earlier observations in humans that treatment with bile acid sequestrants or interruption of enterohepatic bile acid cycling increases hepatic VLDL production (8, 9). Conversely, treatment of subjects with chenodeoxycholic acid ameliorates hypertriglyceridemia and reduces VLDL secretion through mechanisms that include transcriptional repression of *Mttp* (microsomal triglyceride transfer protein) gene expression (10–12). In another approach, treatment of wild type mice

* This work was supported, in whole or in part, by National Institutes of Health Grants R01 DK056260 and R37 HL038180 (to N. O. D.) and P30 DK052574 (to N. O. D. and the Washington University Digestive Diseases Research Core Center, in particular the Morphology and Functional Genomics Cores).

[S] The on-line version of this article (available at http://www.jbc.org) contains supplemental Table 1 and Figs. 1 and 2.

[1] To whom correspondence should be addressed: GI Division, WA University School of Medicine, 660 S. Euclid Ave., St. Louis, MO 63110. E-mail: nod@wustl.edu.

with an FXR agonist both protected against diet-induced gallstones and decreased plasma triglyceride levels (13). Yet other studies demonstrated that mice with liver-specific inactivation of *Mttp* are protected against diet-induced gallstones (14), whereas increased expression of hepatic Mttp was found in humans with cholesterol gallstone disease (15). These findings, coupled with earlier observations suggesting that APOB100 is more susceptible (than APOB48) to presecretory degradation in the setting of limiting *Mttp* expression or function (16, 17), imply the possibility that there may also be an APOB isoform-specific dependence for hepatic lipid mobilization directed toward canalicular secretion.

The current studies were undertaken to examine the importance of *Apobec-1* as a genetic modifier of cholesterol gallstone formation in a congenic strain of C57BL/6 mice, in particular its functional significance in relation to the *Lith6* locus identified earlier (5). In addition, we were intrigued by the findings that mice genetically engineered to express only APOB100 (but which are *Apobec-1*-sufficient (18)) exhibited protection from cholesterol gallstone formation compared with mice expressing only APOB48, predominantly through decreased intestinal cholesterol absorption (19). However, our findings illustrate a divergence in the phenotype demonstrated in that report (19). We find that *Apobec-1*$^{-/-}$ mice demonstrate accelerated gallstone formation and alterations in biliary lipid metabolism that reflect changes in gene expression that are most likely produced by post-transcriptional modifications in *Cyp7a1* mRNA expression.

MATERIALS AND METHODS

Animals and Diets—Apobec-1$^{-/-}$ mice (20) were backcrossed >12 generations onto a C57BL/6 background. Male C57BL/6 wild type (WT)[2] mice were purchased from Jackson Laboratories (Bar Harbor, ME). *Apob*$^{100/100}$ mice were obtained as a generous gift from Dr. Steve Young (UCLA School of Medicine) and are on a mixed background (C57BL/6 and 129/SvJ) (18). All animals were maintained on a 12-h light-dark cycle, in a full barrier facility. 8–10-week-old male *Apobec-1*$^{-/-}$ and WT mice were fed either a standard rodent chow (PicoLab Rodent Diet 20, fat 4.5%, cholesterol 0.015%) or a lithogenic diet (LD) (Research Diet 960393, fat 18.8%, cholesterol 1.2%, and cholic acid 0.5%) for 2–8 weeks, as indicated.

Gallbladder Bile and Gallstone Analysis—Mice were fasted for 4 h and anesthetized with a mixture of ketamine (100 mg/kg) and xylazine (20 mg/kg). Gallbladders were ligated and punctured at the fundus for collection of gallbladder bile. Bile samples were collected and immediately analyzed (2, 21) by polarizing microscopy using a visual scale with the following criteria: 0 = absence of cholesterol monohydrate crystals (ChMCs), 1 = small number of ChMCs (<3/high power field); 2 = many ChMCs (≥3/high power field); 3 = aggregated ChMCs; 4 = presence of "sandy" light translucent stones or "solid" light opaque stones (21).

Bile Flow, Biliary Lipid Output, and Bile Acid Species Determination—Mice were anesthetized as above after a 4-h fast. An external bile fistula was established surgically via the gallbladder fundus. Hepatic bile was collected for up to 60 min while maintaining body temperature at 37 °C. Hepatic bile volume was determined gravimetrically, assuming a density of 1 g/ml. Bile samples were stored at −80 °C until analyzed. Biliary phospholipid, cholesterol, and total bile acid content were determined enzymatically using a phospholipid B kit (catalog number 990-54009), cholesterol E kit (catalog number 439-17501), and total bile acids kit (catalog number 431-15001), respectively, all from Wako Chemicals (Neuss, Germany). Cholesterol saturation indices in hepatic bile were calculated using published parameters (22). Individual bile salt concentrations were measured via high performance liquid chromatography (HPLC) (23). In brief, 100 μl of diluted hepatic bile (1:20 dilution prepared in methanol) was injected onto a Pursuit C18 reverse phase column (Varian, Lake Forest, CA) using a Rainin HPXL HPLC system (Varian, Lake Forest, CA). Bile acid standards were purchased from Steraloids Inc. (Newport, RI) or from Calbiochem. The hydrophobic index of hepatic bile samples was calculated according to published methods (24).

Hepatic and Intestinal Lipid Determination—Animals were sacrificed as described above after a 4-h fast. Liver and mucosal scrapings were collected from the small intestine and frozen at −80 °C until analyzed. Tissue lipids were extracted into chloroform/methanol (2:1), and triglyceride, cholesterol, free fatty acids, and phospholipids were analyzed enzymatically with an L-type triglyceride H kit (catalog number 993-37592, 993-37492), cholesterol E, HR series NRFA-HR(2) (catalog number 995-34691, 995-34791), and phospholipids B, respectively (Wako Chemicals).

Bile Acid Pool Size and Fecal Bile Acid Output Determination—Bile acid pool size was determined as the sum total bile acid content of the entire small intestine, gallbladder, and liver, which were homogenized and extracted together in ethanol with [24-^{14}C]taurocholic acid (0.025 μCi) added as an internal recovery standard (25). Total bile acid mass was determined enzymatically as above. In addition, fecal bile acid output was determined from stool quantitatively collected from individually housed mice for periods up to 72 h. For each determination, 200-mg triplicate aliquots of dried feces were extracted into ethanol as described (25, 26), and total bile acid mass was again measured enzymatically, normalizing recovery to an internal standard of [^{14}C]taurocholic acid.

Cholesterol Absorption—Cholesterol absorption was measured by a fecal dual isotope ratio method, as described previously (27, 28). Wild type and *Apobec-1*$^{-/-}$ mice were studied prior to initiating the lithogenic diet and again after 8 weeks on the lithogenic diet. Animals were gavaged with 150 μl of corn oil mixed with 1 μCi of [^{14}C]cholesterol (PerkinElmer Life Sciences) and 2 μCi of [^{3}H]sitostanol (American Radiolabeled Chemicals, Inc.). Feces were collected individually for 48 h after label administration and processed as previously described. The ratio of ^{14}C and ^{3}H in each sample was determined, and cholesterol absorption percentage was calculated as described previously (27, 29).

[2] The abbreviations used are: WT, wild type; LD, lithogenic diet; HPLC, high performance liquid chromatography; qRT-PCR, quantitative reverse transcription-PCR; UTR, untranslated region; Ad, adenovirus; ChMC, cholesterol monohydrate crystal.

TABLE 1

Body weight, liver weight, serum, and hepatic lipid profile of WT and *Apobec-1*$^{-/-}$ mice on both chow and lithogenic diets

Values represent the mean ± S.E. (*n*). ALT, alanine aminotransferase. mg/g, mg/g of liver.

Parameters	Chow		Lithogenic diet		*p*
	WT	*Apobec-1*$^{-/-}$	WT	*Apobec-1*$^{-/-}$	
Body weight (g)	26.53 ± 0.77 (12)	26.88 ± 0.88 (13)	23.64 ± 0.40 (17)	23.59 ± 0.46 (22)	
Liver wt (g)	1.27 ± 0.04 (12)	1.19 ± 0.03 (13)	1.53 ± 0.05 (18)	1.08 ± 0.03 (22)	$p < 0.01^a$
Liver wt (% body wt)	4.81 ± 0.19 (12)	4.46 ± 0.11 (13)	6.76 ± 0.18 (18)	5.03 ± 0.13 (22)	$p < 0.01^a$
Serum cholesterol (mg/dl)	62.17 ± 2.79 (12)	65.33 ± 3.04 (13)	146.37 ± 5.17 (8)	156.36 ± 7.91 (10)	
Serum triglyceride (mg/dl)	28.43 ± 3.26 (20)	57.05 ± 5.13 (22)	24.43 ± 2.74 (12)	52.84 ± 11.74 (14)	$p < 0.05^a$; $p < 0.05^b$
Serum bile acid (μmol/liter)	6.11 ± 1.21 (4)	6.88 ± 1.10 (5)	16.56 ± 3.28 (8)	22.41 ± 4.46 (10)	
Serum ALT (IU/liter)	10.45 ± 3.97 (7)	15.86 ± 2.59 (8)	59.87 ± 11.04 (8)	49.35 ± 10.30 (14)	
Hepatic cholesterol (mg/g)	1.21 ± 0.06 (5)	1.31 ± 0.09 (5)	19.11 ± 0.91 (12)	15.61 ± 0.64 (15)	$p < 0.01^a$
Hepatic triglyceride (mg/g)	3.71 ± 0.42 (5)	4.86 ± 0.81 (5)	15.67 ± 1.28 (12)	12.73 ± 0.73 (15)	$p < 0.05^a$
Hepatic phospholipid (mg/g)	5.29 ± 0.22 (5)	5.77 ± 0.31 (5)	15.24 ± 0.55 (12)	14.80 ± 0.56 (15)	
Hepatic free fatty acid (μmol/g)	1.05 ± 0.14 (5)	1.45 ± 0.18 (5)	3.76 ± 1.15 (12)	2.91 ± 0.14 (15)	

[a] Comparing WT and *Apobec-1*$^{-/-}$ mice on lithogenic diet.
[b] Comparing WT and *Apobec-1*$^{-/-}$ mice on chow diet.

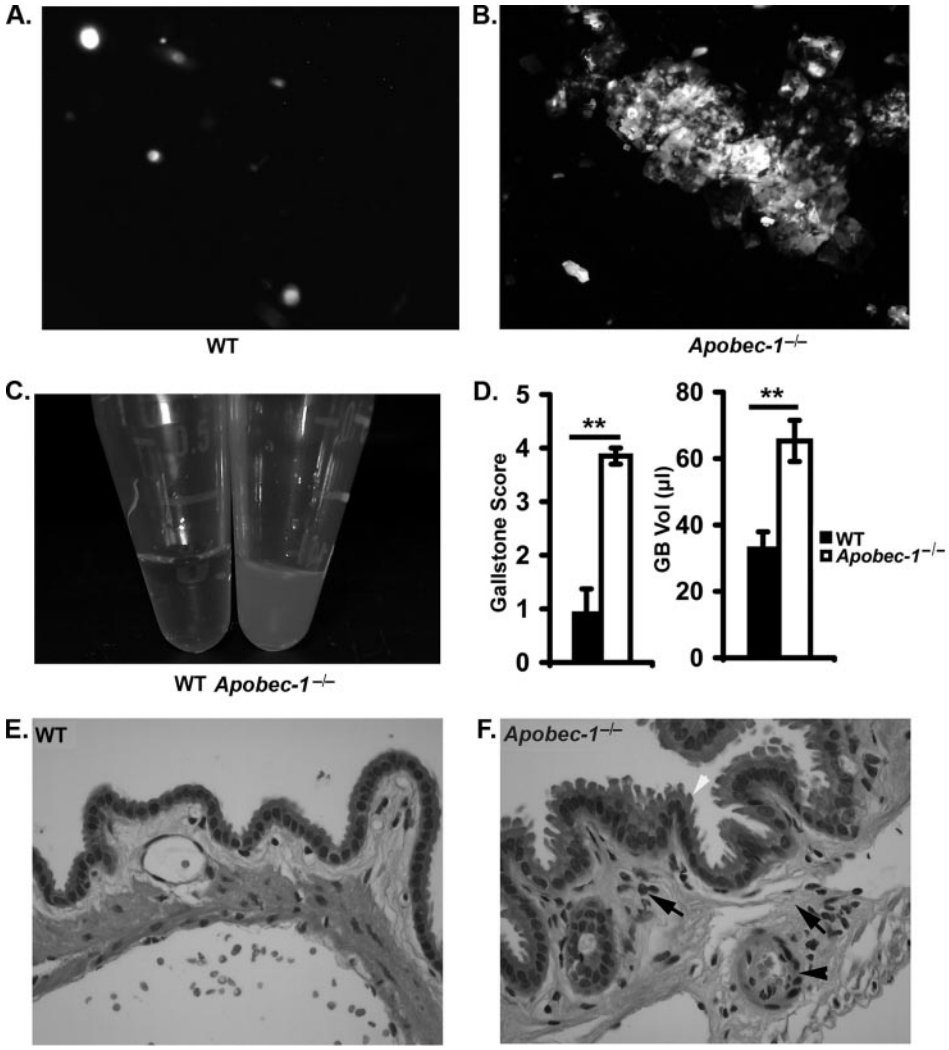

FIGURE 1. **Biliary cholesterol crystallization, gallstone score, and gallbladder inflammation in LD fed wild type and *Apobec-1*$^{-/-}$ mice.** 11 WT and 10 *Apobec-1*$^{-/-}$ mice were fed the LD for 2 weeks. Gallbladder bile samples were collected and analyzed under polarizing microscopy. *A* and *B*, a few single ChMCs were present in WT gallbladder bile (*A*), whereas multiple aggregated ChMCs were observed in gallbladder bile from *Apobec-1*$^{-/-}$ mice (*B*). *C*, gallbladder bile appears turbid in *Apobec-1*$^{-/-}$ compared with WT mice. *D*, gallstone score (see "Materials and Methods") and gallbladder volumes reveal a higher gallstone score and larger gallbladder volume in *Apobec-1*$^{-/-}$ compared with WT mice. *E* and *F*, histological examination of gallbladder epithelium following hematoxylin and eosin staining. The *black arrows* indicate stromal granulocyte infiltration into a thickened gallbladder wall. The *black arrowhead* indicates submucosal vasodilatation. The *white arrowhead* indicates mucosal surface indentations noted in *Apobec-1*$^{-/-}$ but not WT mice (magnification, ×400). **, $p < 0.01$.

Gene Expression Analysis—For microarray analysis, total liver RNA was pooled from 4 animals/group. Pooled RNA was hybridized to an Agilent Technologies mouse whole genome microarray (G4122A; Agilent, Palo Alto, CA). Microarray results were confirmed by real time quantitative reverse transcription-PCR (qRT-PCR) using cDNA pooled from 4 or 5 animals/group, and where indicated, the findings were replicated using individual samples. qRT-PCR assays were performed in triplicate on an ABI Prism 7000 sequence detection system using SYBR Green PCR Master Mix (Applied Biosystems) and primer pairs designed by Primer Express software (Applied Biosystems) (listed in supplemental Table 1). Relative mRNA abundance is expressed as fold change compared with mRNA levels in WT mice consuming the same diet, normalized to 18 S ribosomal RNA. Nuclear run-on assays were performed using isolated nuclei freshly prepared from chow-fed WT ($n = 5$) and *Apobec-1*$^{-/-}$ mice ($n = 5$), purified through sucrose gradients, and frozen in liquid nitrogen until used for run-on studies. Nuclear run-on transcription was performed at 30 °C for 30 min in a mixture containing 5×10^7 nuclei; 5 mM Tris, pH 8.0; 2.5 mM $MgCl_2$, 0.15 M KCl, 1 mM each ATP, CTP, and GTP; 150 μCi of [^{32}P]UTP (3000 Ci/mmol, Amersham Biosciences); and 100 units of RNaseOUT™ (Invitrogen). RNAs were denatured and hybrid-

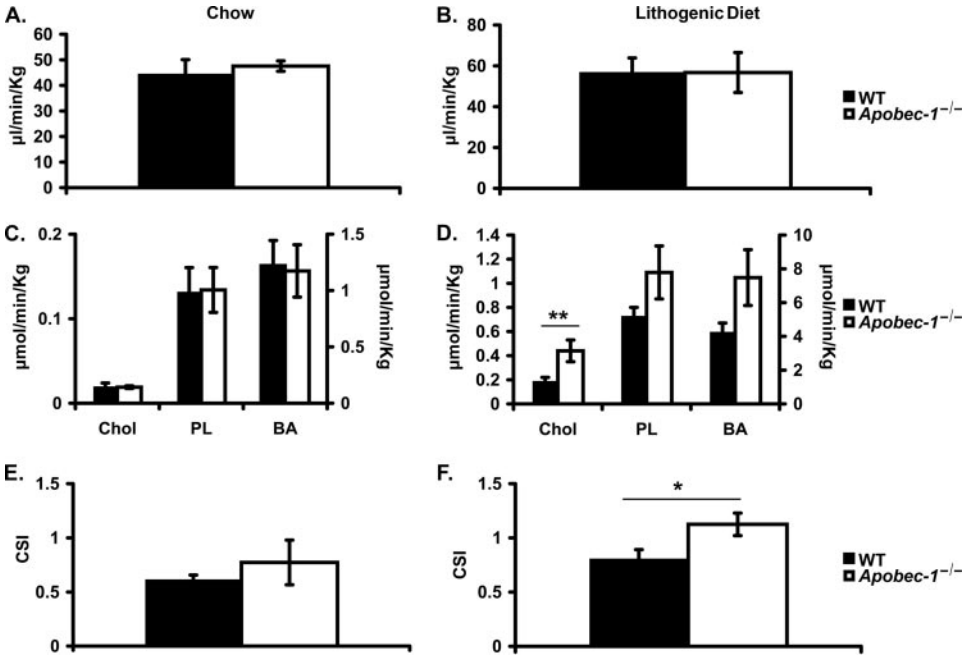

FIGURE 2. **Biliary flow, lipid secretion rates, and hepatic bile cholesterol saturation indices on chow or LD.** Hepatic bile was collected as described for 60 min. *A* and *B*, biliary flow rates (µl/min/kg of body weight) were similar in *Apobec-1*$^{-/-}$ and WT mice either on chow (*A*) or LD diet (*B*). *C* and *D*, biliary cholesterol secretion (µmol/min/kg of body weight) was similar on chow but increased on lithogenic diet in *Apobec-1*$^{-/-}$ mice compared with WT controls. There were no differences in biliary phospholipids or bile acid secretion on either diet between the two genotypes. *E* and *F*, hepatic bile cholesterol saturation indices (*CSI*) were calculated from Carey's critical tables (see "Materials and Methods"). *Apobec-1*$^{-/-}$ mice demonstrated increased CSI on LD but not chow, compared with WT mice. *Bar graphs* indicate the mean ± S.E. Data were from 5 mice/genotype on chow diet and 10 mice/genotype on LD. *, $p < 0.05$; **, $p < 0.01$.

ized to immobilized cDNA templates encoding ~300 bp of *Cyp7a1*, *Gapdh*, or plasmid vector control, washed at high stringency (30, 31), and exposed to PhosphorImager screens (Amersham Biosciences).

Microsome Preparation—Liver microsomes were prepared as described (32). In brief, livers from mice of the indicated genotype were quickly removed and homogenized at 4 °C in buffer I containing 40 mM Tris-HCl, 1 mM EDTA, 5 mM dithiothreitol, 50 mM KCl, 50 mM KF, 300 mM sucrose, and 1× protease inhibitor mixture (Roche Applied Science). The homogenate was centrifuged at 20,000 × *g* for 20 min, and the supernatant was further centrifuged at 108,000 × *g* for 60 min. The pellet was washed and resuspended in buffer II (buffer I without sucrose), and aliquots representing 25 µg of microsomal protein were separated by 8% SDS-PAGE. Western blot was performed on either whole liver homogenate or microsome preparations with affinity-purified rabbit anti-CYP7A1 IgG (2 µg/ml), a generous gift from Dr. Simon Hui (San Diego State University) and as control either anti-BiP IgG (StressGen) or anti-HSP40 followed by ECL detection reagents (Amersham Biosciences).

Plasmid Construction, in Vitro Transcription, and RNA-Protein UV Cross-linking—cDNA from total mouse liver RNA was used to amplify the *Cyp7a1* 3′-untranslated region (UTR). The full-length 3′-UTR was cloned behind a green fluorescent protein cDNA as a reporter for mRNA stability studies using actinomycin D (5 µg/ml), as detailed previously (33). Three individual fragments, collectively spanning the entire *Cyp7a1* 3′-UTR, were used for RNA binding studies. Fragment A spans nucleotides 1642–2314, fragment B spans nucleotides 2287–3274, and fragment C spans nucleotides 3251–4070. Each fragment was cloned into pcDNA3, and the plasmids were linearized and used as templates for *in vitro* transcription with T7 RNA polymerase. *In vitro* transcription reactions were conducted for 6 h with [α-^{32}P]UTP, and the resultant RNA product was gel-purified through 5% PAGE, 7 M urea. ^{32}P-Labeled cRNA template (100,000 cpm) was incubated with 50–1000 ng of glutathione *S*-transferase-APOBEC-1 (34) in a binding buffer containing 10 mM HEPES (pH 7.9), 100 mM KCl, 1 mM EDTA, and 0.25 mM dithiothreitol at room temperature for 15 min. Heparin (3 mg/ml) was then added for another 10 min, and the mixture was digested with RNase T1 (5 units/ml) for another 10 min. The mixture was then subjected to UV cross-linking on ice in a UV Stratalinker 1800 with an energy of 250 mJ/cm^2 and resolved by 10% SDS-PAGE.

Adenovirus Infection in Vivo and Co-immunoprecipitation of RNA-Protein Complexes—Recombinant adenoviruses encoding either rat *Apobec-1* (Ad-Apobec-1) or β-galactosidase (Ad-β-galactosidase) were prepared as described (35), and 6 × 10^8 plaque-forming units were injected into *Apobec-1*$^{-/-}$ mice. 5 days later, animals were anesthetized after a 4-h fast, livers were collected, and *Cyp7a1* expression was examined as described above. For co-immunoprecipitation studies, livers from Ad-Apobec-1-infected *Apobec-1*$^{-/-}$ mice were removed, diced by hand into small (less than 2-mm) pieces, and cross-linked in 1% formaldehyde phosphate-buffered saline complemented with RNaseOUT™ (100 units/ml) and 1× protease inhibitor mixture for 15 min on ice. The cross-link reaction was stopped, and liver pieces were homogenized in 1 ml of polysome lysis buffer containing 10 mM HEPES (pH 7.4), 100 mM KCl, 5 mM $MgCl_2$, 1 mM dithiothreitol, 100 units/ml RNaseOUT™, 1 mmol ribonucleoside vanadyl complex, 0.5% Nonidet P-40. Lysates with 4–5 mg of protein were immunoprecipitated with affinity-purified rabbit anti-APOBEC-1 IgG or control IgG. The RNA-protein complex pellet with protein A beads was treated with proteinase K for 30 min and reverse cross-linked by incubating the mixture at 65 °C for 60 min. RNA from the final pellet was extracted into phenol/choloroform/isoamylcohol and subjected to reverse transcription-PCR for *Cyp7a1* using the primer pairs indicated in supplemental Table 1.

Statistical Analysis—Statistical significance was determined with an unpaired, two-tailed Student's *t* test. Data are expressed as the mean ± S.E. unless otherwise noted.

TABLE 2
Liver microarray data for chow

Gene name	Gene description	Accession number	Ratio[a]	qRT-PCR	*p*
Bile acid synthesis, transport, and metablolism					
Cyp7a1	Cholesterol 7α-hydroxylase	NM_007824	0.17	0.25[b]	0.01
Cyp8b1	Sterol 12α-hydroxylase	NM_010012	0.31	1.15[b]	
Cyp27a1	Sterol 27-hydroxylase	NM_024264	0.65	0.9	
Bsep/Abcb11	Bile salt export pump	NM_021022	0.9	0.75	
Ntcp	Na^+-taurocholate co-transporting protein	NM_011387	0.98	1.42	
Oatp4	Organic anion transporter, 1b2	NM_178235	1.07	1.28	
Oatp2	Organic anion transporter, 1a4	NM_030687	1.5	1.69	
Mdr2/Abcb4	ATP-binding cassette, B4	NM_008830	1.25		
Mrp2/Abcc2	ATP-binding cassette, C2	NM_013806	1.1		
Cyp2b10	Cytochrome P450, 2b10	NM_009998	0.73	2.97	
Cyp3a11	Cytochrome P450, 3a11	NM_007818	0.7	0.51	
Cholesterol synthesis and transport					
Hmgcr	Hydroxymethylglutaryl-CoA reductase	NM_008255	0.7	1.64[b]	
Abca1	ATP-binding cassette, A1	NM_013454	1.4	1	
Abcg5	ATP-binding cassette, G5	NM_031884	1	1.3	
Abcg8	ATP-binding cassette, G8	NM_026180	1	1.5	
Srb1	Scavenger receptor class, B1	NM_016741	1.1	1.28	
Scp2	Sterol carrier protein 2, liver	NM_011327	1.3	0.66	
Lfabp	Liver fatty acid-binding protein	NM_017399	1.2	1.06	
Cav1	Caveolin 1	NM_007616	1.0	1.12	
Npc1	Niemann-Pick type C1	NM_008720	0.9		
Transcription factors or nuclear receptors					
Lxrα	Liver X receptor α	NM_013839	0.81	0.94[b]	
Fxr	Farnesoid X receptor	NM_009108	1.3	1.16	
Shp	Small heterodimer partner	NM_011850	0.66	0.37	
Pparα	Peroxisome proliferator-activated receptor α	NM_011144	1.5	1.6	
Srebp1	Sterol regulatory element-binding protein 1	NM_011480	0.8	0.6[b]	
Srebp2	Sterol regulatory element-binding protein 2	NM_033218	0.99	1.1	
Pxr	Pregnane X receptor	NM_010936	1.2	1.33	
Lrh-1	Liver receptor homolog	NM_030676	0.98		
Fatty acids synthesis and oxidation					
Fasn	Fatty acid synthase	NM_007988	1.1	0.4	
Ucp2	Uncoupling protein 2	NM_011671	1.1	1.03	
Scd1	Stearoyl-coenzyme A desaturase 1	NM_009127	0.9	0.43	
Scd2	Stearoyl-coenzyme A desaturase 2	NM_009128	1.1	0.58	
Acc	Acetyl-coenzyme A carboxylase α	NM_133360	0.9		
Lipoprotein metabolism					
ApoB	Apolipoprotein B	XM_137955	2.06	1.08[b]	
ApoA4	Apolipoprotein A-IV	NM_007468	0.53	0.95	
ApoC3	Apolipoprotein C-III	NM_023114	1.2	0.7	
ApoC2	Apolipoprotein C-II	NM_009695	1	0.92	
Ldlr	Low density lipoprotein receptor	NM_010700	0.65	0.89	
ApoA1	Apolipoprotein A	NM_009692	0.94		
ApoE	Apolipoprotein E	NM_009696	1.2		
Others					
Cyp2C38	Cytochrome P450, 2C38	NM_010002	0.8	0.7	
Cyp4a14	Cytochrome P450, 4A14	NM_007822	1.6	0.4	

[a] Microarray data are expressed as a ratio of *Apobec1*$^{-/-}$ *versus* WT. Relative mRNA expression of some genes was confirmed by real time qRT-PCR by using pooled cDNA (5 mice/group). qRT-PCR results are expressed as -fold change normalized to WT control.
[b] Relative mRNA expression of the indicated genes was confirmed using individual samples ($n = 4$).

RESULTS

Body Weight, Hepatic, and Serum Lipid Profile in LD-fed Apobec-1$^{-/-}$ Mice—Body weight was comparable between the genotypes after 2 weeks of feeding an LD with animals of both genotypes losing weight, but there was a striking decrease in liver weight and liver weight/body weight ratio in *Apobec-1*$^{-/-}$ mice (Table 1). In addition, serum triglyceride levels were 2-fold higher in both chow- and LD-fed *Apobec-1*$^{-/-}$ mice compared with WT with comparable serum cholesterol levels, whereas hepatic cholesterol and triglyceride content were reduced in LD-fed *Apobec-1*$^{-/-}$ mice (Table 1). These findings suggested that LD feeding is accompanied by distinctive alterations in lipid metabolism in *Apobec-1*$^{-/-}$ mice compared with congenic WT controls.

Gallstone Susceptibility Is Increased in LD-fed Apobec-1$^{-/-}$ Mice—To explore the effects on biliary lipid metabolism, samples of gallbladder bile from LD-fed animals were analyzed by polarizing microscopy, which revealed the presence of abundant aggregated birefringent cholesterol crystals in samples from *Apobec-1*$^{-/-}$ mice (Fig. 1*B*) but not in WT samples (Fig. 1*A*). In addition, bile samples from *Apobec-1*$^{-/-}$ mice were grossly turbid (Fig. 1*C*) in comparison with WT controls, and by 2 weeks of LD feeding there were visible stones in 90% of *Apobec-1*$^{-/-}$ mice (9 of 10 mice) compared with 16% (2 of 12) WT controls. This increased susceptibility to gallstones in *Apobec-1*$^{-/-}$ mice was evident also in both the higher gallstone score and increased gallbladder volumes (Fig. 1*D*). In addition, the gallbladder mucosa of LD-fed *Apobec-1*$^{-/-}$ mice appeared thickened histologically, with increased inflammatory cell infiltration (Fig. 1, *E* and *F*).

Alterations in Biliary Lipid Secretion in LD-fed Apobec-1$^{-/-}$ Mice—The findings to this point strongly suggest that *Apobec-1*$^{-/-}$ mice exhibit a striking phenotype of increased gallstone susceptibility upon LD feeding. We next examined individual

TABLE 3
Liver microarray data for lithogenic diet for 2 weeks

Gene name	Gene description	Accession number	Ratio[a]	qRT-PCR	*p*
Bile acid synthesis, transport, and metablolism					
Cyp7a1	Cholesterol 7α-hydroxylase	NM_007824	0.16	0.04[b]	0.001
Cyp8b1	Sterol 12α-hydroxylase	NM_010012	0.36	0.07	0.01
Cyp27a1	Sterol 27-hydroxylase	NM_024264	0.82	0.9	
Bsep/Abcb11	Bile salt export pump	NM_021022	2.89	1.74	
Ntcp	Na^+-taurocholate co-transporting protein	NM_011387	1.7	0.63	
Oatp4	Organic anion transporter, 1b2	NM_178235	2.01	0.48	
Oatp2	Organic anion transporter, 1a4	NM_030687	3.49	2.55	
Mdr2/Abcb4	ATP-binding cassette, B4	NM_008830	1.3	0.87	
Mrp2/Abcc2	ATP-binding cassette, C2	NM_013806	1.13		
Cyp2b10	Cytochrome P450, 2b10	NM_009998	5	19.56	
Cyp3a11	Cytochrome P450, 3a11	NM_007818	2.5	4.29	
Cholesterol synthesis and transport					
Hmgcr	Hydroxymethylglutaryl-CoA reductase	NM_008255	2.09	1.84[b]	0.04
Abca1	ATP-binding cassette, A1	NM_013454	2.1	1.1	
Abcg5	ATP-binding cassette, G5	NM_031884	1.6	1.03[b]	
Abcg8	ATP-binding cassette, G8	NM_026180	1.01	1.03	
Srb1	Scavenger receptor class, B1	NM_016741	1.6	0.89	
Scp2	Sterol carrier protein 2, liver	NM_011327	2.1	1.71	
Lfabp	Liver fatty acid binding protein	NM_017399	2.3	1.32	
Cav1	Caveolin 1	NM_007616	1.8	0.69	
Npc1	Niemann-Pick type C1	NM_008720	1.2		
Transcription factors or nuclear receptors					
Lxrα	Liver X receptor α	NM_013839	0.88	0.53[b]	
Fxr	Farnesoid X receptor	NM_009108	2.05	1.3	
Shp	Small heterodimer partner	NM_011850	0.93	1.4	
Pparα	Peroxisome proliferator-activated receptor α	NM_011144	2.1	1.1	
Srebp1	Sterol regulatory element-binding protein 1	NM_011480	3.64	0.91[b]	
Srebp2	Sterol regulatory element-binding protein 2	NM_033218	0.61	0.83	
Pxr	Pregnane X receptor	NM_010936	1.7	2.25	
Lrh-1	Liver receptor homolog	NM_030676	1.6		
Fatty acid synthesis and oxidation					
Fasn	Fatty acid synthase	NM_007988	8.1	15.1	
Ucp2	Uncoupling protein 2	NM_011671	0.46	0.13	
Scd1	Stearoyl-coenzyme A desaturase 1	NM_009127	1.6	2.07	
Scd2	Stearoyl-coenzyme A desaturase 2	NM_009128	2.0	1.56	
Acc	Acetyl-coenzyme A carboxylase α	NM_133360	2.0		
Lipoprotein metabolism					
ApoB	Apolipoprotein B	XM_137955	1.45	0.91[b]	
ApoA4	Apolipoprotein A-IV	NM_007468	2.45	2.4	
ApoC3	Apolipoprotein C-III	NM_023114	2.45	1.16	
ApoC2	Apolipoprotein C-II	NM_009695	2.43	0.84	
Ldlr	Low density lipoprotein receptor	NM_010700	0.8	1.83	
ApoA1	Apolipoprotein A	NM_009692	1.0		
ApoE	Apolipoprotein E	NM_009696	1.2		
Others					
Cyp2C38	Cytochrome P450, 2C38	NM_010002	4.9	1	
Cyp4a14	Cytochrome P450, 4A14	NM_007822	122.8	372.2	

[a] Microarray data are expressed as a ratio of *Apobec1$^{-/-}$ versus* WT. Relative mRNA expression of some genes was confirmed by real time qRT-PCR by using pooled cDNA (5 mice/group). qRT-PCR results are expressed as -fold change normalized to WT control.
[b] Relative mRNA expression of indicated genes was confirmed using individual samples ($n = 4$).

biliary lipid secretion rates in WT and *Apobec-1$^{-/-}$* mice both on chow and LD. The findings reveal comparable bile flow rates in both genotypes on both diets (Fig. 2, *A* and *B*) and comparable secretion rates of all biliary lipid classes in chow-fed mice (Fig. 2*C*). The secretions of phospholipids and bile acids were also comparable in both genotypes on both diets. By contrast, 2 weeks of LD feeding produced an increase in biliary cholesterol secretion in *Apobec-1$^{-/-}$* mice (Fig. 2*D*), which was accompanied by an increase in cholesterol saturation index that was not observed in chow-fed mice (Fig. 2, *E* and *F*).

Changes in Hepatic Gene Expression in Apobec-1$^{-/-}$ Mice in Response to LD Feeding—In order to begin to understand the complex adaptations that might lead to the increased cholesterol secretion and accelerated formation of gallstones in *Apobec-1$^{-/-}$* mice, we turned to microarray analysis of hepatic gene expression in animals consuming either chow or LD. The most significant alterations encountered in chow-fed mice are summarized in Table 2, and those for LD-fed animals are summarized in Table 3. Among the most striking findings is that chow-fed *Apobec-1$^{-/-}$* mice demonstrate a 75% decrease in *Cyp7a1* mRNA, which encodes the first and rate-limiting enzyme in bile acid synthesis (Table 2). In response to LD feeding, the changes in *Cyp7a1* were further magnified (Table 3), suggesting a profound suppression in bile acid synthesis in response to the dietary intervention. There was a nonsignificant trend to increased *Apobec-1* mRNA in WT mice following 2 weeks LD feeding (2.7 ± 0.8-fold) and no significant differences in *Abcg5* or *Abcg8* mRNA abundance or in other canalicular or basolateral cholesterol transporter mRNAs, including *Srb1* and *Abca1* between WT and *Apobec-1$^{-/-}$* mice (Table 3). Thus, the most striking alterations in gene expression in LD-fed *Apobec-1$^{-/-}$* mice appear to center around genes regulating bile acid synthesis rather than cholesterol secretion. We will return to this observation below.

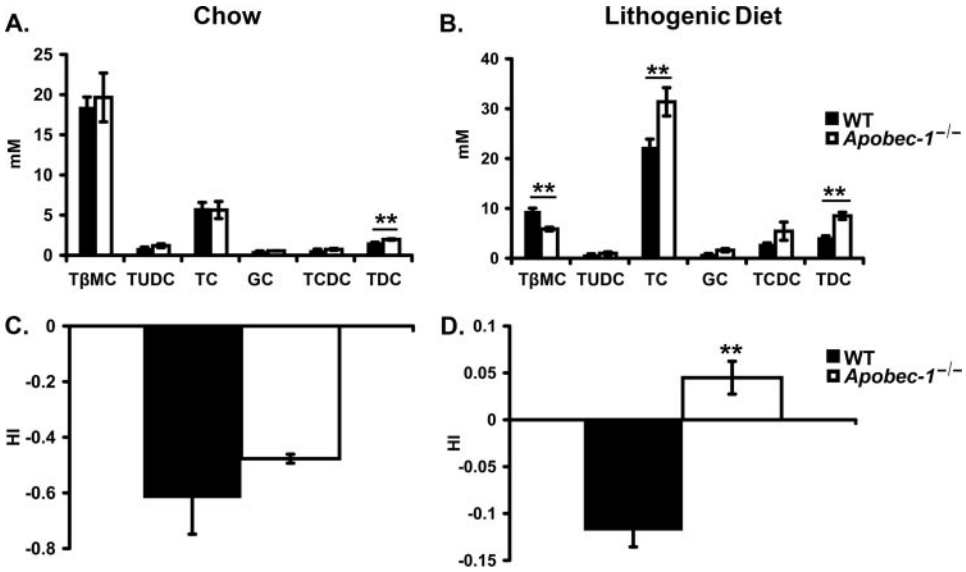

FIGURE 3. **Bile acid species distribution and hydrophobicity index.** Individual bile acid species were examined in newly secreted bile samples from mice fed chow (*A*) (n = 5/genotype) or lithogenic diet (*B*) (n = 7/genotype) by HPLC. *Bar graphs* represent the mean ± S.E. *TβMC*, tauro-β-muricholate; *TUDC*, tauroursodeoxycholate; *TC*, taurocholate; *GC*, glycocholate; *TCDC*, taurochenodeoxycholate; *TDC*, taurodeoxycholate. Bile salt hydrophobicity indices were comparable in chow-fed animals (*C*) but increased in *Apobec-1*$^{-/-}$ mice *versus* WT controls mice when fed the LD (*D*). **, $p < 0.01$.

Alterations in Biliary Bile Acid Composition and Hydrophobicity in Apobec-1$^{-/-}$ *Mice*—Individual species of biliary bile acid were examined by HPLC, which demonstrated that the primary bile acids β-muricholate and taurocholate together represent the dominant species in chow-fed animals of both genotypes (Fig. 3*A*), with an increase in taurodeoxycholic acid observed in *Apobec-1*$^{-/-}$ mice. In response to LD feeding, there was a shift in the bile acid species, with taurocholate representing 58.6 ± 2.2% of the pool in *Apobec-1*$^{-/-}$ mice compared with 54.7 ± 1.3% in WT controls and a corresponding decrease in β-muricholate to 11.3 ± 0.9% in *Apobec-1*$^{-/-}$ mice compared with 23.5 ± 1.1% in WT controls (Fig. 3*B*). In addition, there was a further increase in the relative abundance of taurodeoxycholic acid in *Apobec-1*$^{-/-}$ mice (Fig. 3*B*). The changes in bile acid composition upon LD feeding were accompanied by alterations in the hydrophobic index of bile. Although comparable values were found in chow-fed animals (Fig. 3*C*), there was a significant increase in hydrophobicity noted in *Apobec-1*$^{-/-}$ mice upon LD feeding (Fig. 3*D*). These findings suggest that the combination of increased cholesterol secretion and increased bile hydrophobicity might accelerate cholesterol supersaturation in the bile of *Apobec-1*$^{-/-}$ mice.

Bile Acid Pool Size and Synthetic Rates in Apobec-1$^{-/-}$ *Mice*—We observed a significant 31% decrease in the total bile acid pool size in chow-fed *Apobec-1*$^{-/-}$ mice (Fig. 4*A*), but fecal bile acid excretion rates (at steady state, a surrogate for bile acid synthesis rates) revealed no statistically significant difference between the genotypes (WT 9.2 ± 3.1 μmol/100 g of body weight/day *versus* 7.9 ± 2.1 μmol/100 g of body weight/day; Fig. 4*B*, *left*). The S.D. of these values (25–33%) probably preclude detection of subtle (albeit significant) changes in bile acid excretion rates in chow-fed WT *versus Apobec-1*$^{-/-}$ mice. By contrast, upon feeding the LD, we observed a 1.4-fold increase in the bile acid pool size in *Apobec-1*$^{-/-}$ mice, which was accompanied by a significant 32% decrease in fecal bile acid output (Fig. 4, *A* and *B*). The combination of an expanded bile acid pool (largely the result of dietary cholate supplementation) in the setting of reduced fecal losses suggests the possibility that enterohepatic bile acid recycling may be increased in *Apobec-1*$^{-/-}$ mice. As an initial approach to address this possibility, we examined the expression of *Asbt*, the ileal bile salt transporter mRNA, and found that it was increased 2.5-fold in LD-fed *Apobec-1*$^{-/-}$ mice (Fig. 4*C*). These findings collectively suggest that there is adaptive conservation of bile acids (predominantly of dietary origin) resulting from up-regulation of ileal *Asbt* expression in *Apobec-1*$^{-/-}$ mice.

Cholesterol Absorption and Sterol Transporter Expression in Apobec-1$^{-/-}$ *Mice*—Previous studies examining gallstone susceptibility in the background of hepatic and intestinal production of APOB100-only lipoproteins were undertaken in mice, where the synthesis of APOB48 was eliminated through *Apob* gene targeting, a mechanism independent of C to U RNA editing (18). In this setting, *Apob*$^{100/100}$ mice were found to be protected against diet-induced gallstones in conjunction with a dramatic reduction in intestinal cholesterol absorption (19). Accordingly, we reasoned that cholesterol absorption might be correspondingly altered in the APOB100-only background associated with *Apobec-1* deletion. To our surprise, however, this was not the case. Our findings demonstrate that (percentage) cholesterol absorption was indistinguishable in chow-fed wild type and *Apobec-1*$^{-/-}$ mice, although somewhat lower in LD-fed *Apobec-1*$^{-/-}$ mice compared with wild type controls (26 ± 0.5% *versus* 33 ± 2%; Fig. 5*A*, *right*). Since these findings were so divergent from those reported in *Apob*$^{100/100}$ mice (19) (expanded discussion below), we undertook our own examination of cholesterol absorption in the APOB100-only (*Apobec-1* wild type) background, yet again, our findings demonstrated no alteration in cholesterol absorption in either genotype when the mice were fed a chow diet and, equally surprisingly, revealed no differences when these *Apob*$^{100/100}$ mice consumed the LD (Fig. 5*B*). Taken together, these findings suggest that the increased susceptibility to gallstone formation noted in *Apobec-1*$^{-/-}$ mice is unlikely to be attributed to increased cholesterol absorption. Furthermore, our findings fail to confirm the previously documented decrease in cholesterol absorption in both chow and LD-fed *Apob*$^{100/100}$ mice (19).

Decreased Cyp7a1 Gene Expression in Apobec-1$^{-/-}$ *Mice*—Since the most striking effects noted in this study were related to the alterations in bile acid metabolism, we asked whether the decreased expression of *Cyp7a1* mRNA in *Apobec-1*$^{-/-}$ mice (Fig. 6, *A* and *B*) was accompanied by a corresponding decrease

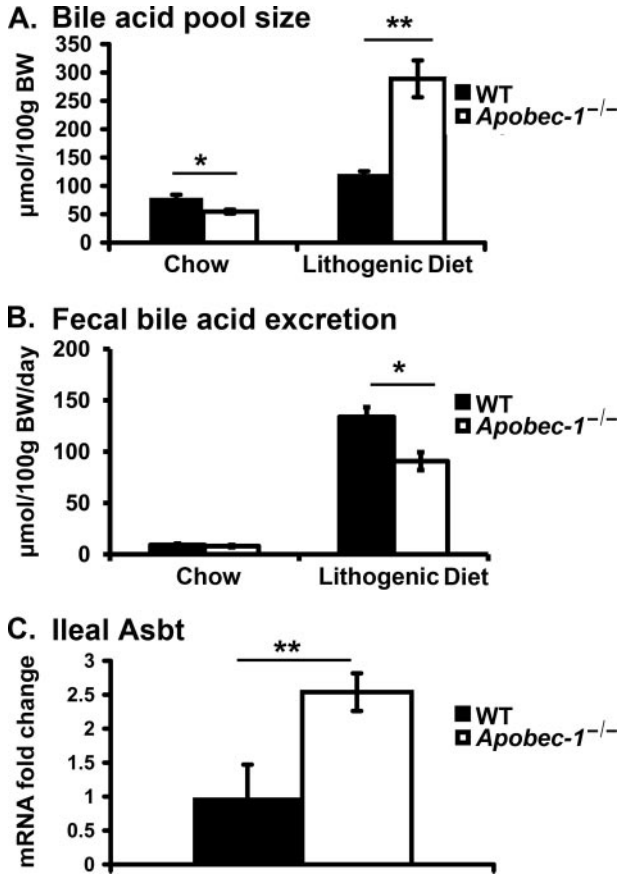

FIGURE 4. **Bile acid pool size, fecal bile acid excretion, and ileal *Asbt* (apical sodium-dependent bile acid transporter) mRNA expression.** *A*, bile acid pool size (μmol/100 g of body weight) was decreased in *Apobec-1*$^{-/-}$ mice on a chow diet but increased in *Apobec-1*$^{-/-}$ mice fed an LD for 2 weeks. Liver, gallbladder, and intestine were pooled and subjected to ethanolic bile acid extraction. Total bile acid mass was measured enzymatically. *B*, fecal bile acid excretion was comparable in chow-fed mice of both genotypes, but LD-fed *Apobec-1*$^{-/-}$ mice excrete less bile acid than WT controls. Mice were individually housed, and feces were collected up to 72 h. Fecal bile acids were extracted and quantitated enzymatically. *C*, *Asbt* mRNA abundance is increased in LD-fed *Apobec-1*$^{-/-}$ mice. RNA was extracted from ileum of LD-fed WT and *Apobec-1*$^{-/-}$ mice, and *Asbt* expression was measured by qRT-PCR. *Bar graphs* represent the mean ± S.E. from 5 mice/genotype on chow and 4 mice/genotype on LD. *, $p < 0.05$; **, $p < 0.01$.

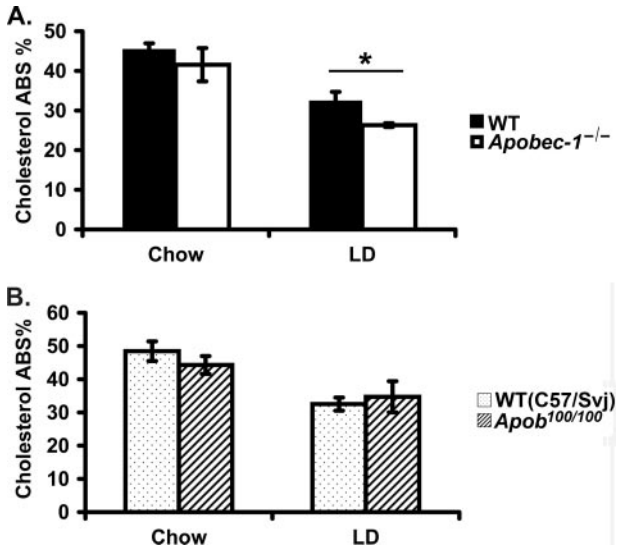

FIGURE 5. **Cholesterol absorption in *Apobec-1*$^{-/-}$ mice and in *Apob*$^{100/100}$ mice.** *A*, cholesterol absorption in mice of the indicated genotype fed either chow or LD for 8 weeks was measured by fecal dual isotope ratio methodology. There was similar cholesterol absorption in *Apobec-1*$^{-/-}$ mice and WT controls on the chow diet, but cholesterol absorption was decreased in *Apobec-1*$^{-/-}$ mice fed the LD. *Bar graphs* show the mean ± S.E. of data from 8 mice/genotype on chow and 4 mice/genotype on LD. *B*, cholesterol absorption was similar in *Apob*$^{100/100}$ mice and control (*C57/129Svj*) mice either on chow or LD for 8 weeks. *Bar graphs* show the mean ± S.E., 5 mice/genotype for each study. *, $p < 0.05$.

in protein expression. We found decreased microsomal CYP7A1 protein in chow-fed *Apobec-1*$^{-/-}$ mice and virtually undetectable levels when *Apobec-1*$^{-/-}$ mice were fed the LD (Fig. 6*C*). These findings together point to an unanticipated adaptation in *Apobec-1*$^{-/-}$ mice in which *Cyp7a1* expression is markedly attenuated in chow-fed animals and further suppressed following LD feeding.

Post-transcriptional Modulation of Cyp7a1 Gene Expression in Apobec-1$^{-/-}$ *Mice; APOBEC-1 Binds Cyp7a1 RNA in Vitro and in Vivo*—To pursue the mechanisms of the decrease in *Cyp7a1* gene expression, we first turned to nuclear run-on analysis to examine whether *Cyp7a1* gene transcription was decreased. Our findings revealed no change in *Cyp7a1* transcription in nuclei from chow-fed wild type and *Apobec-1*$^{-/-}$ mice (Fig. 7*A*). These results suggested the possibility that APOBEC-1 modulates posttranscriptional regulation of *Cyp7a1* gene expression. Accordingly, we examined the possibility that APOBEC-1, an RNA-binding protein with affinity for AU-rich targets beyond *ApoB* mRNA (33, 36), might exhibit RNA binding activity toward the *Cyp7a1* 3′-UTR, a region of the transcript that contains a large number of AU-rich motifs and the UUUN(A/U)U consensus site for APOBEC-1 binding (36) (Fig. 7*B*). Recombinant APOBEC-1 was demonstrated to bind to each of the three fragments of murine *Cyp7a1* 3′-UTR (Fig. 7*B*), and binding was competed by excess unlabeled competitor (supplemental Fig. 1). Endogenous *Cyp7a1* mRNA expression was significantly increased in HepG2 cells following adenovirus-mediated *Apobec-1* infection, although a small nonspecific effect (statistically insignificant) was observed following Ad-β-galactosidase transduction (Fig. 7*C*). We further demonstrated that APOBEC-1 binds *Cyp7a1* mRNA *in vivo*, following immunoprecipitation of Ad-Apobec-1 hepatic lysates with anti-APOBEC-1 IgG, which revealed the presence of *Cyp7a1* RNA in the immune pellet (Fig. 7*D*). This approach was necessary, since APOBEC-1 is a low abundance protein, and co-immunoprecipitation experiments with anti-APOBEC-1 IgG in hepatic lysates from WT animals failed to reveal *Cyp7a1* RNA. In addition, control co-immunoprecipitation experiments in nontransduced or Ad-β-galactosidase-transduced *Apobec-1*$^{-/-}$ mice were negative (data not shown).

Ad-Apobec-1 Rescues Cyp7a1 Gene Expression in Vivo—In order to demonstrate more directly that APOBEC-1 might modify *Cyp7a1* gene expression, we examined the consequences of Ad-Apobec-1 rescue in chow-fed Apobec-1$^{-/-}$ mice. This approach revealed a ~10-fold increase in *Cyp7a1* mRNA abundance (Fig. 7*E*, *top*), suggesting that *Apobec-1* repletion indeed results in increased *Cyp7a1* gene expression. We found that injection of control adenovirus also increased *Cyp7a1* mRNA expression, but the increase was significantly lower than with Ad-Apobec-1 (Fig. 7*E*). These differences were

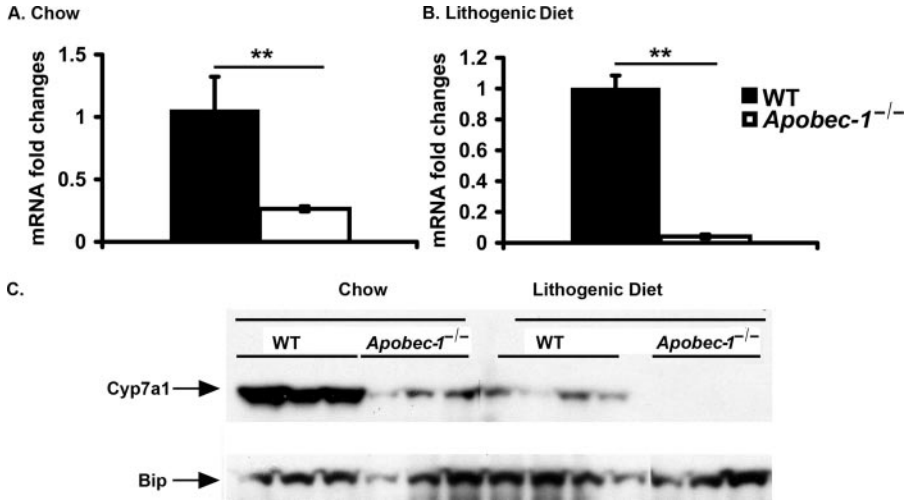

FIGURE 6. **Decreased hepatic Cyp7a1 mRNA and protein expression in chow-fed *Apobec-1*$^{-/-}$ mice and a further decrease in LD-fed mice.** *A*, relative expression of hepatic *Cyp7a1* mRNA in chow-fed mice. *Bar graphs* show the mean ± S.E. of data from four WT and five *Apobec-1*$^{-/-}$ mice. *B*, relative expression of hepatic *Cyp7a1* mRNA in LD-fed mice. *Bar graphs* show the mean ± S.E. of data from three WT and five *Apobec-1*$^{-/-}$ mice. *C*, Western blot analysis of CYP7A1 protein expression in liver microsomes prepared as described from chow or LD-fed animals. 25 μg of protein was subjected to SDS-PAGE and Western blotted with anti-CYP7A1 IgG and anti-BIP IgG. 3–4 mice from each genotype were studied.

even more dramatically illustrated when CYP7A1 protein expression was examined (Fig. 7*E*, *bottom*). In addition, Ad-Apobec-1 administration decreased *Cyp8b1* mRNA (1.04 (no Ad) *versus* 1.73 (Ad-β-galactosidase) *versus* 0.37 (Ad-Apobec-1)) (Fig. 7*E*), findings consistent with a compensatory down-regulation following rescue of *Cyp7a1* expression.

We attempted to pursue the gain-of-function effects of APOBEC-1 on RNA turnover using chimeric green fluorescent protein-reporter constructs cloned upstream of the full-length murine *Cyp7a1* 3′-UTR, expressed in a variety of cell lines (including HepG2, COS, HeLa, and HEK; data not shown). Steady-state green fluorescent protein mRNA abundance was 2.5-fold greater in the absence of the *Cyp7a1* 3′-UTR (supplemental Fig. 2*A*), results similar to those noted in other studies (37). These findings suggest that the 3′-UTR of *Cyp7a1* contains destabilizing elements. However, using actinomycin D-treated HepG2 cells, we were unable to show an effect of Ad-Apobec-1 on mRNA half-life of either the endogenous *Cyp7a1* or of a chimeric green fluorescent protein-3′-UTR (data not shown), similar to earlier reports suggesting that actinomycin D inhibits a factor(s) required for *Cyp7a1* mRNA decay (38). Accordingly, we turned to an alternative approach to examine mRNA decay using transcriptional pulsing in tet-off cells (39). Although this approach revealed that the murine *Cyp7a1* 3′-UTR conferred instability to a chimeric reporter transcript (supplemental Fig. 2*B*), there was no effect of *Apobec-1* transfection (supplemental Fig. 2*C*), suggesting that the effects noted *in vivo* cannot be readily modeled in a cell culture system. We will discuss the implications of these particular findings below.

DISCUSSION

The findings herein demonstrate a dramatic phenotype of increased gallstone susceptibility in *Apobec-1*$^{-/-}$ mice induced by feeding a lithogenic diet. The suggestion that Apobec-1 expression might be linked to gallstone susceptibility emerged from quantitative trait locus mapping, in which a locus on the middle to distal region of chromosome 6 displayed linkage in D2 × CAST intercrosses, raising the possibility that alterations in hepatic APOB isoforms might in turn lead to alterations in biliary lipid secretion (2, 21). Our *a priori* objective in initiating these studies was to examine in more detail the role of *Apobec-1*, in particular to understand the possible pathways by which alterations in the production of APOB isoforms might conceivably lead to changes in canalicular lipid secretion. Our findings demonstrate alterations in bile acid pool size and composition, which, combined with increased biliary cholesterol secretion, increase bile lithogenicity in *Apobec-1*$^{-/-}$ mice. The current findings, however, are in stark contrast to the phenotype reported in *Apob*$^{100/100}$ mice where these animals were protected against diet-induced gallstones (19). Furthermore, and also somewhat unexpectedly, our findings suggest that *Cyp7a1* gene expression is reduced in *Apobec-1*$^{-/-}$ mice, most likely at a post-transcriptional level. Several elements of these findings and our attempts to resolve the underlying mechanisms bear additional discussion.

The first and most striking finding was the increased susceptibility to diet-induced gallstones in *Apobec-1*$^{-/-}$ mice. In particular, there was a significant 2-fold increase in biliary cholesterol secretion in LD-fed *Apobec-1*$^{-/-}$ mice, whose basis is not completely explained. We found no change in hepatic mRNA expression for any of several candidate genes implicated in biliary cholesterol transport (including *Abcg5/g8*, *Abca1*, and *Srb1*), although we did not systematically evaluate protein expression or localization of these genes. This caveat notwithstanding, it is possible that the increased cholesterol secretion may reflect alterations in metabolic trafficking rather than changes in the expression of transporter genes. In support of this possibility is the finding that hepatic cholesterol content was decreased in LD-fed *Apobec-1*$^{-/-}$ mice compared with wild type controls. We also examined the possibility that intestinal absorption of cholesterol might be altered, particularly since studies in *Apob*$^{100/100}$ mice demonstrated a dramatic reduction in cholesterol absorption in LD-fed mice, from ~52% in wild type mice to ~9% in the *Apob*$^{100/100}$ background (19). Those studies also reported that biliary cholesterol secretion was decreased ~2-fold in LD-fed *Apob*$^{100/100}$ mice (19). However, both findings contrast with our results in LD-fed *Apobec-1*$^{-/-}$ mice. We found no differences in cholesterol absorption in chow-fed wild type and *Apobec-1*$^{-/-}$ mice, although there was a small, albeit significant, reduction in cholesterol absorption in LD-fed *Apobec-1*$^{-/-}$ mice. Moreover, we observed no differences in cholesterol absorption in either chow or LD-fed

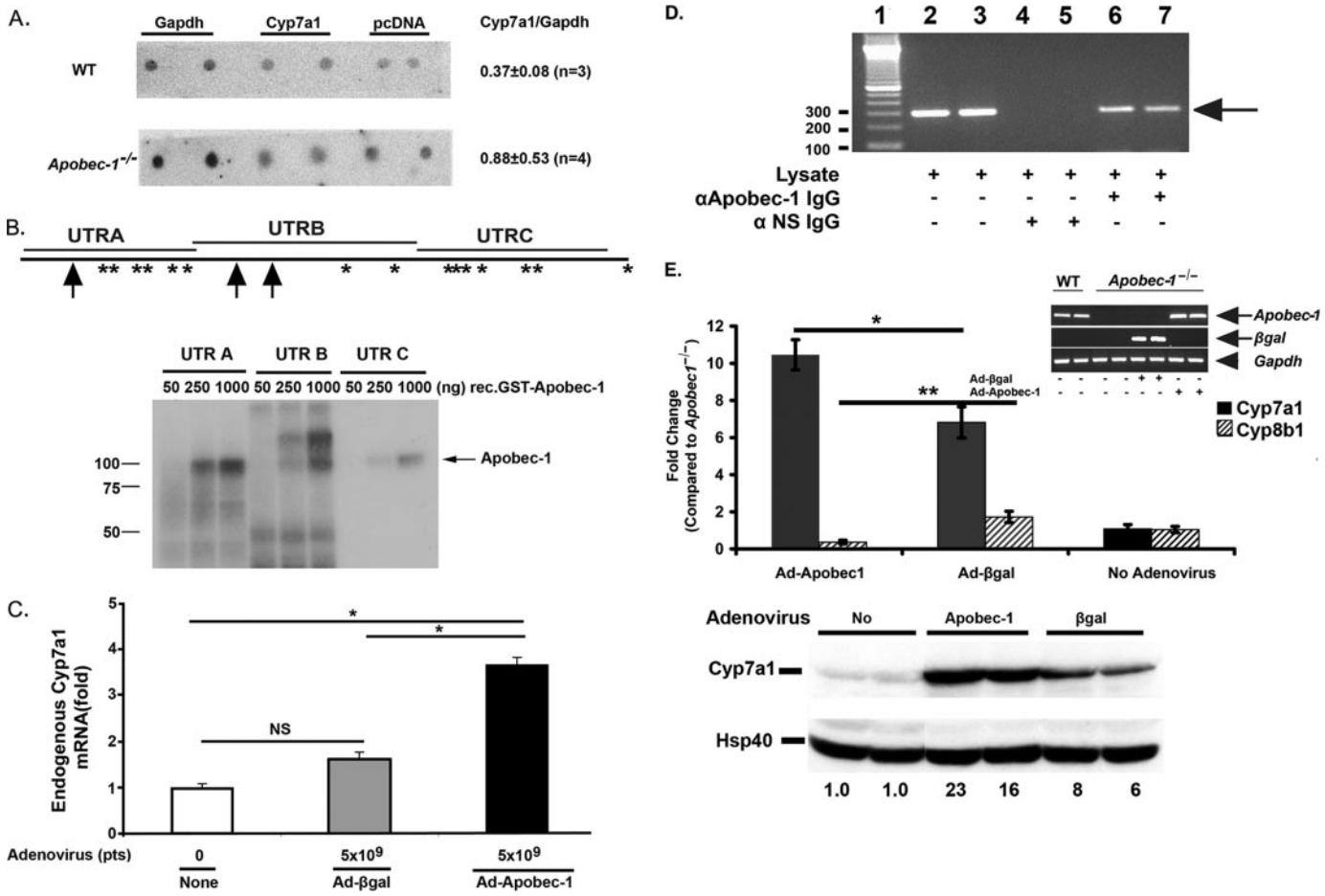

FIGURE 7. **Apobec-1-dependent modulation of Cyp7a1 gene expression.** *A*, nuclear run-on assays show similar *Cyp7a1* transcription rate in *Apobec-1*$^{-/-}$ and WT mice. Isolated nuclei were prepared from two separate groups ($n = 4$ or 5 mice/group for each experiment) of WT and *Apobec-1*$^{-/-}$ mice and run-on transcripts hybridized to immobilized DNA encoding *Gapdh*, *Cyp7a1*, or pcDNA3.1 for background control. Radiolabeled nascent RNA hybridizing to *Cyp7a1 versus Gapdh* was determined by phosphorimaging and corrected for background control. The data are derived from 3–4 independent experiments from mice of the indicated genotype. The quantitation is indicated on the *right* as the mean ± S.E. *B*, *top*, distribution of Apobec-1 binding sites UUUN(A/U)U in Cyp7a1 3′-UTR is shown. Schematic representation of Apobec-1 binding motif in 3′-UTR of murine *Cyp7a1*. *, single copy APOBEC-1 binding motif. *Arrow*, two tandem repeats of APOBEC-1 binding motif. *Cyp7a1* 3′-UTR was divided into three different fragments (UTRA, UTRB, and UTRC) whose coordinates are detailed under "Materials and Methods." *Bottom*, UV-cross-linking assays were performed with radiolabeled cRNA (UTRA, UTRB, or UTRC) and 50–1000 ng of glutathione *S*-transferase-APOBEC-1. Molecular mass makers are shown on the *left*. The *arrow* indicates the cross-linked bands. *C*, *Apobec-1* transfection increases endogenous *Cyp7a1* mRNA expression in HepG2 cells. HepG2 cells were infected with 5×10^9 particles (*pts*) of Ad-β-galactosidase or Ad-Apobec-1 for 48 h. *Cyp7a1* mRNA expression was determined by quantitative PCR. Data are normalized to *Cyp7a1* mRNA expression in noninfected HepG2 cells. *Bar graphs* represent the mean ± S.E. from 2–4 independent assays. *, $p < 0.05$ in the groups of transduced and untransduced HepG2 cells. *D*, *Cyp7a1* mRNA can be coimmunoprecipitated with anti-APOBEC-1 IgG. Liver lysates were freshly prepared from *Apobec-1*$^{-/-}$ mice following infection with Ad-Apobec-1 and immunoprecipitated with anti-APOBEC-1 IgG or control IgG. RNA was extracted from the immune pellet (or input lysate in *lanes 2* and *3*) and subjected to reverse transcription-PCR with primers specific to *Cyp7a1*. The *arrow* indicates the *Cyp7a1* amplified bands. Molecular mass makers are shown on the *left*. *NS*, nonspecific IgG. *E*, hepatic *Cyp7a1* mRNA expression (*top*) and protein expression (*bottom*) in *Apobec-1*$^{-/-}$ mice was increased by Ad-Apobec-1 infection. By contrast, Ad-Apobec-1 infection decreased *Cyp8b1* mRNA expression in *Apobec1*$^{-/-}$ mice. Relative expression of hepatic *Cyp7a1* and *Cyp8b1* mRNA was analyzed by qRT-PCR. Data are normalized to hepatic *Cyp7a1* or *Cyp8b1* expression of *Apobec-1*$^{-/-}$ mice without adenovirus infection. *Bar graphs* show mean ± S.E., 5 mice/group. *Filled bar*, *Cyp7a1*; *hatched bar*, *Cyp8b1*. The *inset images* confirm comparable *Apobec-1* mRNA expression (reverse transcription-PCR) following Ad-Apobec-1 delivery or of β-galactosidase mRNA expression following Ad-β-galactosidase delivery into *Apobec-1*$^{-/-}$ liver. The *arrows* indicate *Apobec-1* or β-galactosidase-specific RT-PCR products, and the *arrowhead* indicates *Gapdh*-specific RT-PCR product. *, $p < 0.05$; **, $p < 0.01$. Hepatic CYP7A1 protein expression was analyzed by Western blot and quantitated by imaging, with HSP40 used as a loading control. The *numbers below* each *lane* indicate relative abundance of CYP7A1 after normalizing expression to uninfected *Apobec-1*$^{-/-}$ mice (no adenovirus) as 1.

Apob$^{100/100}$ mice compared with controls. It is worth emphasizing that although the data presented in Fig. 5 suggest that the percentage absorption of cholesterol tended to decrease in animals of all genotypes fed the LD, the net intestinal cholesterol mass absorbed is vastly increased in the cholate-supplemented, LD-fed animals, as evidenced by the dramatic increase in hepatic cholesterol content (Table 1). That said, our findings provide no support for the proposal that ApoB100-only mice, either in the *Apobec-1*$^{-/-}$ background or *Apob*$^{100/100}$ background (*Apobec-1*-sufficient), exhibit a discernable difference in cholesterol absorption on either diet. We can only speculate on the reasons for the discrepancy in the *Apob*$^{100/100}$ background, but subtle differences in strain, bacterial colonization, or other environmental modifiers may be relevant considerations.

We further report heretofore unanticipated alterations in bile acid metabolism in *Apobec-1*$^{-/-}$ mice and a striking decrease in the expression of *Cyp7a1*, the enzyme regulating the initial step in the microsomal bile acid synthetic pathway. There was a ~75% decrease in *Cyp7a1* gene expression in

chow-fed *Apobec-1*$^{-/-}$ mice accompanied by a small yet statistically significant decrease (31%) in the bile acid pool size. We found no differences in fecal bile acid excretion despite the decrease in *Cyp7a1* mRNA expression in chow-fed *Apobec-1*$^{-/-}$ mice, but it is worth noting that fecal bile acid output was only decreased by 60% in *Cyp7a1*$^{-/-}$ mice (25), suggesting that compensatory mechanisms attenuate the net effects on bile acid production, through alternative pathways of bile acid production. The functional implications for bile acid metabolism in chow-fed *Apobec-1*$^{-/-}$ mice are probably modest, since there was no developmental phenotype in terms of fat malabsorption or skin defects comparable with that observed in *Cyp7*$^{-/-}$ mice, although it is worth noting that the heterozygous *Cyp7*$^{+/-}$ mice in those studies were phenotypically normal (40, 41). On the other hand, there was an exaggerated decrease in Cyp7a1 expression in LD-fed *Apobec-1*$^{-/-}$ mice coupled with an increased bile acid pool (as noted above, probably the result of dietary cholate supplementation), decreased fecal bile acid excretion, and a ~2.5-fold increase in ileal Asbt mRNA expression. The mechanisms underlying the change in Asbt mRNA expression in *Apobec-1*$^{-/-}$ mice will require additional study, but the findings suggest that enterohepatic bile acid cycling is increased in LD-fed *Apobec-1*$^{-/-}$ mice, a possibility consistent with the trend toward increased bile acid secretion noted in LD-fed *Apobec-1*$^{-/-}$ mice. Taken together, the results demonstrate a range of alterations in bile acid metabolism, including changes in bile acid species and hydrophobicity that probably contribute to the observed increase in gallstone susceptibility in LD-fed *Apobec-1*$^{-/-}$ mice.

Among the most intriguing questions posed by this study is the mechanism whereby *Cyp7a1* gene expression is modulated in the setting of *Apobec-1* deletion. The finding that RNA transcription rates were comparable in wild type and *Apobec-1*$^{-/-}$ mice most plausibly suggests that the decreased *Cyp7a1* expression in *Apobec-1*$^{-/-}$ mice reflects a post-transcriptional mechanism. We have previously demonstrated that APOBEC-1 binds AU-rich RNA templates, particularly those containing the high affinity consensus sequence (UUUN(A/U)U) embedded within its canonical target *ApoB* RNA as well as others, including c-*Myc* and *Cox-2*, and demonstrated that APOBEC-1 binding to these RNA templates also modulates mRNA stability (33, 36). Other work has established a strong precedent for posttranscriptional regulation of *Cyp7a1* mRNA, and several authors have pointed out the short half-life (~30 min to 1 h) of *Cyp7a1* mRNA both in cell culture (42) and *in vivo* in rat (43–45) and hamster liver (46). In particular, the 3′-UTR of murine (as well as human and rat) *Cyp7a1* contains several AUUUA motifs, which are characteristic of short lived mRNAs (37, 38, 47). These findings led us to speculate that alteration in *Cyp7a1* mRNA stability might account for the changes observed in *Apobec-1*$^{-/-}$ mice. Nevertheless, we were unable to confirm this prediction experimentally using a gain-of-function approach in HepG2 and other cell lines with (either plasmid- or adenovirus-mediated) *Apobec-1* delivery and in models comparing endogenous (*i.e.* human) *Cyp7a1* expression as well as with reporter mRNA constructs cloned in front of the murine *Cyp7a1* 3′-UTR, using both actinomycin D and transcriptional pulsing to examine mRNA decay.

Previous studies demonstrated that dexamethasone treatment induced a posttranscriptional >20-fold increase in steady-state *Cyp7a1* mRNA abundance in L-35 rat hepatoma cells (38). A tetracycline-regulated transcriptional pulsing approach, however, was needed to demonstrate differences in *Cyp7a1* mRNA stability, since treatment of L-35 cells with transcriptional inhibitors (such as actinomycin D) obscured differences in mRNA decay, implicating a labile protein(s) for the dexamethasone-dependent increase in *Cyp7a1* mRNA stability (38). Although we did not attempt to replicate our findings in this clone of rat hepatoma L-35 cells, one possible explanation for our failure to demonstrate a gain-of-function effect of *Apobec-1* on *Cyp7a1* mRNA stability *in vitro* is that the composition, function, or abundance of *Apobec-1*-interacting proteins (including *Acf* (*Apobec-1* complementation factor)) differs in mouse liver and HepG2 cells. Indirect support for this speculation is that some of these *Apobec-1*-interacting proteins (such as *Apobec-1* complementation factor and HuR) bind *Cyp7a1* mRNA,[3] although it remains to be determined whether such binding has physiological relevance. In addition, a number of studies have shown that APOBEC-1-mediated C to U *ApoB* RNA editing requires optimal stoichiometric proportions of *trans*-acting proteins (34, 48), supporting the prediction that the composition of RNA-binding proteins (some of which may be distinctive to murine hepatocytes) that target murine *Cyp7a1* mRNA may in turn be critical determinants of mRNA stability *in vivo*. Another possibility is that *Apobec-1*-dependent modulation of *Cyp7a1* mRNA expression is mediated indirectly, for example via alterations in micro-RNA expression, which again may differ in regulation or composition between HepG2 cells and murine liver. Further study will clearly be required to resolve these crucial questions.

In conclusion, the current findings raise implications for the regulation of *Cyp7a1* gene expression and the integrated role of RNA-binding proteins, including those like *Apobec-1* and its partners, which were originally thought to have a restricted function in C to U RNA editing. The range of alternative targets for these gene products continues to evolve.

Acknowledgment—We acknowledge with gratitude the contributions, discussion, and input of Dr. Malcolm Lyons during the initiation of this study.

REFERENCES

1. Sandler, R. S., Everhart, J. E., Donowitz, M., Adams, E., Cronin, K., Goodman, C., Gemmen, E., Shah, S., Avdic, A., and Rubin, R. (2002) *Gastroenterology* **122,** 1500–1511
2. Lyons, M. A., and Wittenburg, H. (2006) *Gastroenterology* **131,** 1943–1970
3. Zanlungo, S., Rigotti, A., and Nervi, F. (2004) *Curr. Opin. Lipidol.* **15,** 279–286
4. Lammert, F., Carey, M. C., and Paigen, B. (2001) *Gastroenterology* **120,** 221–238
5. Lyons, M. A., Wittenburg, H., Li, R., Walsh, K. A., Leonard, M. R., Korstanje, R., Churchill, G. A., Carey, M. C., and Paigen, B. (2003) *J. Lipid Res.* **44,** 1763–1771
6. Teng, B., Burant, C. F., and Davidson, N. O. (1993) *Science* **260,**

[3] V. Blanc and N. O. Davidson, unpublished observations.

1816–1819
7. Davidson, N. O., and Shelness, G. S. (2000) *Annu. Rev. Nutr.* **20,** 169–193
8. Angelin, B., Einarsson, K., Hellström, K., and Leijd, B. (1978) *J. Lipid Res.* **19,** 1017–1024
9. Angelin, B., Einarsson, K., Hellström, K., and Leijd, B. (1978) *J. Lipid Res.* **19,** 1004–1016
10. Miller, N. E., and Nestel, P. J. (1974) *Lancet* **2,** 929–931
11. Watanabe, M., Houten, S. M., Wang, L., Moschetta, A., Mangelsdorf, D. J., Heyman, R. A., Moore, D. D., and Auwerx, J. (2004) *J. Clin. Invest.* **113,** 1408–1418
12. Hirokane, H., Nakahara, M., Tachibana, S., Shimizu, M., and Sato, R. (2004) *J. Biol. Chem.* **279,** 45685–45692
13. Moschetta, A., Bookout, A. L., and Mangelsdorf, D. J. (2004) *Nat. Med.* **10,** 1352–1358
14. Amigo, L., Castro, J., Miquel, J. F., Zanlungo, S., Young, S., and Nervi, F. (2006) *Gastroenterology* **131,** 1870–1878
15. Castro, J., Amigo, L., Miquel, J. F., Gälman, C., Crovari, F., Raddatz, A., Zanlungo, S., Jalil, R., Rudling, M., and Nervi, F. (2007) *Hepatology* **45,** 1261–1266
16. Wang, Y., McLeod, R. S., and Yao, Z. (1997) *J. Biol. Chem.* **272,** 12272–12278
17. Kulinski, A., Rustaeus, S., and Vance, J. E. (2002) *J. Biol. Chem.* **277,** 31516–31525
18. Farese, R. V., Jr., Véniant, M. M., Cham, C. M., Flynn, L. M., Pierotti, V., Loring, J. F., Traber, M., Ruland, S., Stokowski, R. S., Huszar, D., and Young, S. G. (1996) *Proc. Natl. Acad. Sci. U. S. A.* **93,** 6393–6398
19. Wang, H. H., and Wang, D. Q. (2005) *Hepatology* **42,** 894–904
20. Hirano, K., Young, S. G., Farese, R. V., Jr., Ng, J., Sande, E., Warburton, C., Powell-Braxton, L. M., and Davidson, N. O. (1996) *J. Biol. Chem.* **271,** 9887–9890
21. Lyons, M. A., Wittenburg, H., Li, R., Walsh, K. A., Churchill, G. A., Carey, M. C., and Paigen, B. (2003) *J. Lipid Res.* **44,** 953–967
22. Carey, M. C. (1978) *J. Lipid Res.* **19,** 945–955
23. Rossi, S. S., Converse, J. L., and Hofmann, A. F. (1987) *J. Lipid Res.* **28,** 589–595
24. Heuman, D. M. (1989) *J. Lipid Res.* **30,** 719–730
25. Schwarz, M., Russell, D. W., Dietschy, J. M., and Turley, S. D. (1998) *J. Lipid Res.* **39,** 1833–1843
26. Setchell, K. D., Lawson, A. M., Tanida, N., and Sjövall, J. (1983) *J. Lipid Res.* **24,** 1085–1100
27. Wang, D. Q., Paigen, B., and Carey, M. C. (2001) *J. Lipid Res.* **42,** 1820–1830
28. Wang, D. Q., and Carey, M. C. (2003) *J. Lipid Res.* **44,** 1042–1059
29. Xie, Y., Newberry, E. P., Young, S. G., Robine, S., Hamilton, R. L., Wong, J. S., Luo, J., Kennedy, S., and Davidson, N. O. (2006) *J. Biol. Chem.* **281,** 4075–4086
30. Paulauskis, J. D., and Sul, H. S. (1989) *J. Biol. Chem.* **264,** 574–577
31. Shiels, B. R., Northemann, W., Gehring, M. R., and Fey, G. H. (1987) *J. Biol. Chem.* **262,** 12826–12831
32. Straka, M. S., Junker, L. H., Zacarro, L., Zogg, D. L., Dueland, S., Everson, G. T., and Davis, R. A. (1990) *J. Biol. Chem.* **265,** 7145–7149
33. Anant, S., Murmu, N., Houchen, C. W., Mukhopadhyay, D., Riehl, T. E., Young, S. G., Morrison, A. R., Stenson, W. F., and Davidson, N. O. (2004) *Gastroenterology* **127,** 1139–1149
34. Blanc, V., Navaratnam, N., Henderson, J. O., Anant, S., Kennedy, S., Jarmuz, A., Scott, J., and Davidson, N. O. (2001) *J. Biol. Chem.* **276,** 10272–10283
35. Blanc, V., Henderson, J. O., Newberry, R. D., Xie, Y., Cho, S. J., Newberry, E. P., Kennedy, S., Rubin, D. C., Wang, H. L., Luo, J., and Davidson, N. O. (2007) *Cancer Res.* **67,** 8565–8573
36. Anant, S., and Davidson, N. O. (2000) *Mol. Cell. Biol.* **20,** 1982–1992
37. Agellon, L. B., and Cheema, S. K. (1997) *Biochem. J.* **328,** 393–399
38. Baker, D. M., Wang, S. L., Bell, D. J., Drevon, C. A., and Davis, R. A. (2000) *J. Biol. Chem.* **275,** 19985–19991
39. Chen, C. Y., Yamashita, Y., Chang, T. C., Yamashita, A., Zhu, W., Zhong, Z., and Shyu, A. B. (2007) *RNA* **13,** 1775–1786
40. Ishibashi, S., Schwarz, M., Frykman, P. K., Herz, J., and Russell, D. W. (1996) *J. Biol. Chem.* **271,** 18017–18023
41. Schwarz, M., Lund, E. G., Setchell, K. D., Kayden, H. J., Zerwekh, J. E., Björkhem, I., Herz, J., and Russell, D. W. (1996) *J. Biol. Chem.* **271,** 18024–18031
42. Pandak, W. M., Stravitz, R. T., Lucas, V., Heuman, D. M., and Chiang, J. Y. (1996) *Am. J. Physiol. Gastroentest. Liver Physiol.* **270,** G401–410
43. Ness, G. C., Pendleton, L. C., Li, Y. C., and Chiang, J. Y. (1990) *Biochem. Biophys. Res. Commun.* **172,** 1150–1156
44. Hylemon, P. B., Gurley, E. C., Stravitz, R. T., Litz, J. S., Pandak, W. M., Chiang, J. Y., and Vlahcevic, Z. R. (1992) *J. Biol. Chem.* **267,** 16866–16871
45. Li, Y. C., Wang, D. P., and Chiang, J. Y. (1990) *J. Biol. Chem.* **265,** 12012–12019
46. Feingold, K. R., Spady, D. K., Pollock, A. S., Moser, A. H., and Grunfeld, C. (1996) *J. Lipid Res.* **37,** 223–228
47. Noshiro, M., Nishimoto, M., and Okuda, K. (1990) *J. Biol. Chem.* **265,** 10036–10041
48. Sowden, M. P., Ballatori, N., Jensen, K. L., Reed, L. H., and Smith, H. C. (2002) *J. Cell Sci.* **115,** 1027–1039
49. Yamasaki, S., Stoecklin, G., Kedersha, N., Simarro, M., and Anderson, P. (2007) *J. Biol. Chem.* **282,** 30070–30077